PROC. OF JSCE
No. 296, April 1980

LABORATORY STUDY ON SEDIMENT TRANSPORT MECHANISM DUE TO WAVE ACTION

By Tomoya SHIBAYAMA and Kiyoshi HORIKAWA***

1. INTRODUCTION

Surface waves travelling in shallow water over a sandy bed usually produce back and forth sand movement. The pattern of the movement is classified into two types : bed load movement and suspended load movement. When suspension is marked, sand ripples are usually present and strong vortices are generated on both sides of the ripples. These vortices are considered to be one of the main factors in producing sand suspension over a rippled bed.

Inman[5] studied the ripple formation due to waves and suggested that suspended sand clouds are important factor in considering sediment transport. Inman and Bowen[17] demonstrated that there is an offshore sand transport as suspended load due to ripple asymmetry and the resulting differences in intensity of the vortices. Tunstall and Inman[15] treated energy dissipation due to vortices by oscillatory flow over a wavy boundary using standing vortex theory. Sunamura, Bando and Horikawa[13] carefully observed sand movement over a rippled bed using a 16 mm high speed motion analysis camera and suggested that the movement of the suspended sand clouds is one of the main factors in producing net sediment transport. Yamaguchi and Sawamoto[16] studied motion of the vortices above a rippled bed using potential flow theory and estimated the suspended sediment concentration above such a bed. Nakato et al.[9] examined the mechanism of sediment suspension from a rippled bed and measured the suspended sediment concentration.

Madsen and Grant[8] determined an empirical relationship between a nondimensional average bed load transport rate due to wave action and the Shields parameter using a quasi-steady application of the Einstein-Brown unidirectional flow sediment transport relationship. Sleath[12] measured the quantities of sand moving as bed load over a flat bed.

In order to estimate the net sediment transport rate, Horikawa, Sunamura and Shibayama[4] classified the sediment transport mechanism due to laboratory wave action into four types as below.

Type 1. No suspended sand cloud exists. Bed load transport is dominant. Net sediment transport is in the onshore direction.

Type 2. Suspended sand clouds are formed. Both bed load transport and suspended sand transport should be considered. Net sediment transport direction may be onshore or offshore depending on the dominance of the sediment transport mode.

Type 3. Suspended sand clouds are formed. Suspended sand transport is dominant. Suspended sand clouds are formed only on the onshore sides of ripples. Net sediment transport is in the offshore direction.

Type 4. Suspended sand clouds are formed. Suspended sand transport is dominant. Suspended sand clouds are formed both on the onshore and offshore sides of the ripples. Net sediment transport is in the offshore direction.

In the present study the vortex circulation, the movement of vortex center and the resultant velocity field are considered to predict the sand movement over ripples due to wave action. The amount of suspended sand over ripples are considered using the information of vortex circulation and sand movement in order to estimate suspended sand transport rate. Then formulae describing net sediment transport are proposed for each transport type by applying the suspended sand transport formula presented in this paper and the Madsen and Grant bed load formula.

2. SAND MOVEMENT OVER RIPPLES DUE TO WAVE ACTION

(1) Velocity field over rippled bed due to wave action

The model is based on the complex potential the-

* M. Eng., Postgraduate, Department of Civil Engineering, University of Tokyo.
** Dr. Eng., Professor of Civil Engineering, University of Tokyo.

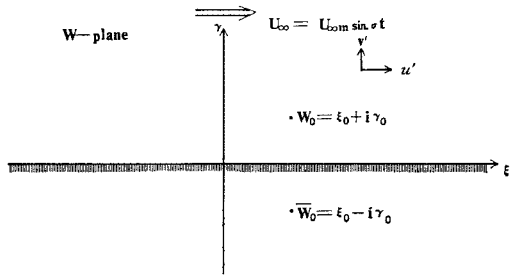

Fig. 1 Definition sketch for flat boundary.

ory. First we consider an oscillatory flow parallel to the real axis with two vortices; one is a real vortex and the other is an image vortex, located at (ξ_0, γ_0) and $(\xi_0, -\gamma_0)$ respectively as shown in **Fig. 1**. These locations are also indicated by the complex numbers $W_0=\xi_0+i\gamma_0$ and $\overline{W}_0=\xi_0-i\gamma_0$. The velocity potential Ω for this model is

$$\Omega=U_\infty W+\frac{\Gamma}{2\pi}i\ln\frac{W-W_0}{W-\overline{W}_0} \quad \cdots\cdots(1)$$

where $W=\xi+i\gamma$, Γ is vortex circulation and U_∞ is the oscillatory flow free stream velocity.

During the first half period, when the free flow velocity is in the positive direction, the circulation Γ of the real vortex was given by Yamaguchi and Sawamoto[16] as the integral of the vorticity flux,

$$\begin{aligned}\Gamma(t)&=K'\int_0^t\int_0^\infty u'\left(\frac{\partial u'}{\partial\gamma}-\frac{\partial v'}{\partial\xi}\right)d\gamma\,dt\\&=K'\int_0^t\frac{1}{2}(K''U_\infty)^2dt\\&=K'''U_{\infty m}{}^2\left(t-\frac{1}{2\sigma}\sin 2\sigma t\right)\quad 0\leqq t\leqq T/2\end{aligned} \quad \cdots\cdots(2)$$

in which

$u'=\xi$-component of fluid velocity;
$v'=\gamma$-component of fluid velocity;
σ=radian wave frequency;
T=period of oscillation;
$K'''=K'K''^2/4$=constant

and

$$U_\infty=U_{\infty m}\sin\sigma t$$

The circulation dissipation is now introduced into this model so that the modeled value agrees with the laboratory data. Differentiation of Equation (2) and adding the dissipation term $-k_2\Gamma$ gives

$$\frac{d\Gamma}{dt}=k_1U_{\infty m}{}^2\sin^2\sigma t-k_2\Gamma \quad \cdots\cdots(3)$$

With the initial condition $\Gamma(0)=0$, the solution of Equation (3) is

$$\begin{aligned}\Gamma(t)=&\frac{k_1U_{\infty m}{}^2}{2k_2}(1-e^{-k_2t})-\frac{k_1U_{\infty m}{}^2}{2(k_2{}^2+4\sigma^2)}\\&\cdot(k_2\cos 2\sigma t+2\sigma\sin 2\sigma t-k_2e^{-k_2t})\end{aligned} \quad \cdots\cdots(4)$$

for $0\leqq t\leqq T/2$.

During the next half period, the circulation is assumed to decrease as follows so that the modeled value agrees with the laboratory data.

$$\begin{aligned}\Gamma(t)&=\left\{\Gamma\left(\frac{T}{2}\right)\right\}e^{-k_3(t-T/2)}\\&=\left\{\frac{k_1U_{\infty m}{}^2}{2k_2}(1-e^{-k_2T/2})-\frac{k_1U_{\infty m}{}^2}{2(k_2{}^2+4\sigma^2)}\right.\\&\quad\left.\cdot(k_2-k_2e^{-k_2T/2})\right\}e^{-k_3(t-T/2)}\end{aligned} \quad \cdots\cdots(5)$$

The complex velocity is derived from Equation (1) as

$$\begin{aligned}\frac{d\Omega}{dW}&=u'-iv'\\&=U_\infty+\frac{\Gamma}{2\pi}i\left(\frac{1}{W-W_0}-\frac{1}{W-\overline{W}_0}\right)\end{aligned} \quad \cdots\cdots(6)$$

Equation (6) can be broken down into real and imaginary parts to obtain the velocity components in the W-plane. We have

$$\left.\begin{aligned}u'&=U_\infty+\frac{\Gamma}{2\pi}\left(\frac{\gamma-\gamma_0}{(\xi-\xi_0)^2+(\gamma-\gamma_0)^2}\right.\\&\quad\left.-\frac{\gamma+\gamma_0}{(\xi-\xi_0)^2+(\gamma+\gamma_0)^2}\right)\\v'&=\frac{\Gamma}{2\pi}\left(\frac{-(\xi-\xi_0)}{(\xi-\xi_0)^2+(\gamma-\gamma_0)^2}\right.\\&\quad\left.+\frac{\xi-\xi_0}{(\xi-\xi_0)^2+(\gamma+\gamma_0)^2}\right)\end{aligned}\right\} \quad \cdots\cdots(7)$$

In order to obtain the movement of the real vortex, we now introduce velocity due to the image vortex located in $\overline{W}_0$ only. The complex potential function $\tilde{\Omega}$ for the resulting flow is given by

$$\tilde{\Omega}=U_\infty W-\frac{\Gamma}{2\pi}i\ln(W-\overline{W}_0)$$

The velocity components $\tilde{u}'$, $\tilde{v}'$ are

$$\tilde{u}'-i\tilde{v}'=U_\infty-\frac{\Gamma}{2\pi}i\frac{1}{W-\overline{W}_0}$$

Hence the velocity components of the point W_0 are given by

$$\left.\begin{aligned}\tilde{u}_0'&=U_\infty-\frac{\Gamma}{4\pi\gamma_0}\\\tilde{v}_0'&=0\end{aligned}\right\} \quad \cdots\cdots(8)$$

The location of the vortex center is determined by Equations (4), (5) and (8). We have

$$\xi_0(t)=\int_0^t\tilde{u}_0'dt+\text{constant}$$

$$=\left\{\begin{aligned}&\frac{U_{\infty m}}{\sigma}(1-\cos\sigma t)-\frac{1}{4\pi\gamma_0}\left\{\frac{k_1U_{\infty m}{}^2}{2k_2}\right.\\&\cdot\left(t+\frac{e^{-k_2t}-1}{k_2}\right)-\frac{k_1U_{\infty m}{}^2}{2(k_2{}^2+4\sigma^2)}\\&\left.\cdot\left(\frac{k_2}{2\sigma}\sin 2\sigma t-\cos 2\sigma t+e^{-k_2t}\right)\right\}-C_1\\&\qquad 0\leqq t\leqq T/2\\&\frac{U_{\infty m}}{\sigma}(1-\cos\sigma t)+\frac{1}{4\pi\gamma_0}\left\{\frac{k_1U_{\infty m}{}^2}{2k_2}\right.\\&\cdot\left[(1-e^{-k_2T/2})\frac{e^{-k_3(t-T/2)}}{k_3}\right.\\&\left.\left.-\left(\frac{T}{2}+\frac{1}{k_2}e^{-k_2T/2}-\frac{1}{k_2}+\frac{1}{k_3}-\frac{e^{-k_2T/2}}{k_3}\right)\right]\end{aligned}\right.$$

$$\left\{ -\frac{k_1 U_{\infty m}^2}{2(k_2^2+4\sigma^2)}\left[(k_2-k_2e^{-k_2T/2})\frac{e^{-k_3(t-T/2)}}{k_3} +1-e^{-k_2T/2}-\frac{k_2}{k_3}+\frac{k_2e^{-k_2}}{k_3}\right]-C_1 \quad \frac{T}{2}\leqq t\leqq T \right\} \cdots\cdots(9)$$

$$\tau_0=\text{constant} \cdots\cdots(10)$$

where C_1 is constant.

Tunstall and Inman[15] used the conformal transformation

$$z=f(W)=W+i\alpha e^{ik_TW} \cdots\cdots(11)$$

which maps the W-plane to the Z-plane so that a flat boundary may be transformed into a wavy boundary with amplitude α and wave number k_T as shown in **Fig. 2**. The wavy boundary gives a good approximation to a rippled surface.

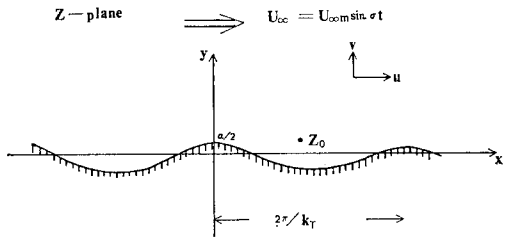

Fig. 2 Definition sketch for wavy boundary.

The components of Equation (11) are

$$\left.\begin{aligned} x&=\xi-\alpha e^{-\gamma k_T}\sin k_T\xi \\ y&=\gamma+\alpha e^{-\gamma k_T}\cos k_T\xi \end{aligned}\right\} \cdots\cdots(12)$$

The complex velocity is transformed as

$$\frac{d\Omega}{dz}=\frac{d\Omega/dW}{dz/dW} =\frac{U_\infty+\dfrac{\Gamma}{2\pi}i\left(\dfrac{1}{W-W_0}-\dfrac{1}{W-\overline{W}_0}\right)}{1-\alpha k_Te^{ik_TW}} =u-iv \cdots\cdots(13)$$

The relation $z=f(W)$ provides a one-to-one conformal transform of the upper W-half-plane into the upper region of the Z-plane. Because of these conditions, the circulation of the vortex is not changed by the mapping. Because $f'(\xi+i\infty)=1$, the value of the velocity at infinity on the Z-plane is the same as that on the W-plane.

From Equations (4), (5), (7), (9) and (10), the velocity field for all time on the W-plane can be calculated. If we give an appropriate initial condition, the pathline of any particle over a rippled bed can be then calculated by using, for example, a Runge-Kutta method and transforming into the Z-plane.

(2) Rate of sand suspension due to wave action

When strong vortices are created on the onshore sides of ripples, suspended sand clouds are formed.

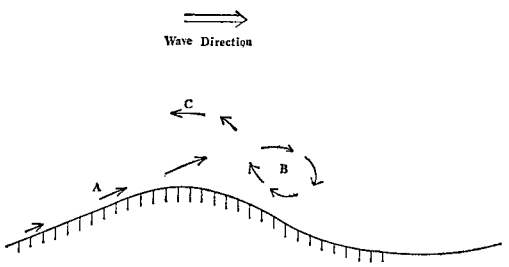

A : Sand is transported along the offshore flank of the ripples
B : Sand forms a suspended sand cloud
C : The cloud is transported in the offshore direction

Fig. 3 Formation of suspended sand cloud.

When the flow velocity is in the onshore direction, sand is transported along the offshore flank of the ripples as bed load movement and then suspended at the crest of the ripples to form a suspended sand cloud as shown in **Fig. 3.** Because of the ripple asymmetry, weak vortices are also created on the offshore sides of ripples. For our purposes, a strong vortex is taken as a circulation is strong enough to produce suspended sand clouds. From now strong vortices are mainly considered.

The amount of sand in the suspended sand cloud will be estimated by a similar method as that used by Madsen and Grant[8] to estimate the bed load transport rate.

For unidirectional steady flow, Brown[1] suggested an empirical relationship

$$\phi=40\,\psi^3$$

$$\psi=\frac{\tau}{(s-1)\rho gd}$$

in which

ϕ=nondimensional sediment transport rate;
ψ=shields parameter;
τ=shear stress;
d=sediment diameter;
ρ=fluid density

and

s=sediment specific gravity.

Madsen and Grant[8] proposed an empirical relationship between the instantaneous dimensionless bed load sediment transport ϕ and the maximum value of the Shields parameter ψ_m as

$$\phi=g_1(\psi_m) \cdots\cdots(14)$$

in which

$$\phi=\frac{q_s}{wd}=\frac{A_s\cdot u_s}{wd} \cdots\cdots(15)$$

$$\psi_m=\frac{\tau_{0m}}{(s-1)\rho gd} \cdots\cdots(16)$$

A_s=amount of moving sand;
q_s=instantaneous volumetric rate of sediment transport;
u_s=sand velocity;

and

w=sand particle fall velocity.

The quantity τ_{0m} is the maximum shear stress given by

$$\tau_{0m}=\frac{1}{2}f_w\rho u_b^2 \quad \cdots\cdots(17)$$

in which f_w is the wave friction factor defined by Jonsson[6] and u_b is the maximum near bottom orbital velocity.

Madsen and Grant used a quasi-steady assumption to Brown's formula and obtained a similar relationship for oscillatory flow based on laboratory data, namely

$$\phi(t)=40\,\psi^3(t) \quad \cdots\cdots(18)$$

We now apply Equation (18) to estimate suspended sand transport. In order to describe the rate at which a particle moves along the offshore flank of a ripple, two empirical observations will be used :

1. A particle moving as bed load will not stop until the flow direction is changed.
2. Sand particles move at almost the same speed as water particles.

We now consider only the time interval $t_i \leqq t \leqq t_e$ during which suspended sand clouds are formed. Symbol t_i indicates the time at which suspended sand cloud starts to be formed and t_e indicates the time at which it stops to increase. For the time interval $t_i \leqq t \leqq T/4$, when sand particles are accelerated, the transport rate is estimated as

$$\phi(t)=40\,\psi^3(t)$$
$$=40\,\psi_m{}^3\sin^6\sigma t \quad \cdots\cdots(19)$$

for

$$\psi(t)=\psi_m\sin^2\sigma t$$

For the time interval $T/4 \leqq t \leqq t_e$, after the amount of moving sand attains maximum, as sand particles once start moving will not stop during the interval and move at the same speed with water particles, which are obtained from the observations mentioned above lead to

$$\phi(t)=\frac{A_{sm}\cdot u(t)}{wd}$$
$$=40\,\psi_m{}^3\sin\sigma t \quad \cdots\cdots(20)$$

in which

A_{sm}=maximum value of amount of moving sand ; and

$u(t)=U_{\infty m}\sin\sigma t$

The time average transport rate is thus estimated to be

$$\bar{\phi}=\frac{2}{T}\left\{\int_{t_i}^{T/4}40\,\psi_m{}^3\sin^6\sigma t dt+\int_{T/4}^{t_e}40\,\psi_m{}^3\sin\sigma t dt\right\}$$
$$=\frac{80}{T}\psi_m{}^3\left[\int_{t_i}^{T/4}\sin^6\sigma t dt+\int_{T/4}^{t_e}\sin\sigma t dt\right]$$
$$=C_2\psi_m{}^3 \quad \cdots\cdots(21)$$

where C_2 is constant.

If we express

$t_i=T/4-\alpha_1 T$

$t_e=T/4+\beta_1 T$

then

$$\bar{\phi}=\frac{80}{T}\psi_m{}^3\left[\int_{T/4-\alpha_1 T}^{T/4}\sin^6\sigma t+\int_{T/4}^{\beta_1 T+T/4}\sin\sigma t dt\right] \quad \cdots\cdots(22)$$

The coefficients α_1 and β_1 could be a function of fluid and bed conditions. For our experiments, under the condition of ripple formation, the coefficients are determined from the laboratory observations.

From the information of the vortex circulation and the sand movement, the suspended sand cloud formation starts at $0.05\,T\sim0.15\,T$ and ends at $0.45\,T\sim0.50\,T$. The constant C_2 varies from 16 to 19. We here put $\alpha_1=0.1$ and $\beta_1=0.25$. Equation (21) becomes

$$\bar{\phi}=18.5\,\psi_m{}^3 \quad \cdots\cdots(23)$$

(3) Experimental procedures and data analysis

The experiments were performed in a wave flume 11 m long, 0.2 m wide and 0.3 m deep. The flume has a hinged plunger type wave generator with which the wave frequency and height can be controlled. The down-wave end of the channel had a porous breakwater installed to absorb the wave energy and decrease reflection. The front side of the flume was made of glass allowing observation of the interior.

In the middle of the flume, a volume of sand was placed 4 cm thick, 80 cm long and 20 cm wide. Sand samples were well-sorted and their median grain size was 0.2 mm.

When waves were generated, sand ripples were formed after 200~300 wave periods. The selection of experimental waves and resultant ripple conditions are shown in **Table 1**. Under these conditions, asymmetrical ripples were formed and strong vortices were generated on the onshore sides of the ripples whereas weak vortices formed on the offshore sides of the ripples. We now consider the strong vortices only.

In order to investigate water particle movement, polystyrene particles of diameter 2 mm or less and specific gravity 1.02 were injected into the water. The movement of sand particles and polystyrene particles over ripples was carefully observed using a

Table 1 Experimental conditions.

Case Number	Wave Period (s)	Wave Height (cm)	Ripple Height (cm)	Ripple Length (cm)
1	0.84	5.8	0.35	3.0
2	1.05	6.5	0.6	4.3
3	1.20	8.3	0.8	5.4
4	1.00	6.0	0.6	3.8
5	1.20	7.6	0.9	5.0
6	1.30	6.0	0.9	5.7
7	1.10	6.5	0.6	4.0

Water depth=16 cm

HITACHI 16 mm high speed motion analysis camera utilizing a film speed of 200~500 frames per second. The relation between the wave phase and the film frame was known by using the HITACHI timing light pulse generator unit with a wave gage. The output of the unit was recorded simultaneously on the film and on the oscillograph paper together with the output of the wave gage.

The dimensions of the vortices and movement of sand and polystyrene particles were obtained by analyzing the 16 mm film using a NAC dynamic frame and screen unit. By means of this unit, the frame number was counted and movement of individual particles was traced on paper.

The water particle velocity field was estimated from the movement of the polystyrene particles, and the circulation of the vortex was determined by integrating the velocity along the closed path which included the vortex center inside. The path was carefully chosen to lie outside of the vortex core given by Tunstall and Inman[15].

The amount of suspended sand was estimated after Sunamura, Bando and Horikawa[13]. The concentration of the suspended sand cloud was measured by a KENEK suspended sand concentration meter which optically measured the suspended sand concentration. The output of the meter was recorded on the oscillograph paper together with the output of the wave gage. The cross-sectional area of the cloud was determined from the 16 mm film pictures. From the product of the concentration and the cross-sectional area of the cloud, the amount of suspended sand could be estimated.

(4) Laboratory results

The vortex circulation and vortex center movement are calculated with the model presented in the previous section. The constants k_1, k_2 and k_3 in Equations (4) and (5) are determined so that the calculated circulation agrees with the measured one. The determined values for k_1, k_2 and k_3 for each case are shown in **Table 2**. Comparisons between measured and modeled values of vortex circulation for Cases 1 and 4 are shown in **Figs. 4** and **5** respectively.

Table 2 Coefficients for circulation model and laboratory results.

Case Number	k_1	k_2	k_3	$U_{\infty m}$ (cm/s)	Γ_{max} (cm²/s)	C_m (ppm×10³)	A (cm²)
1	0.75	0.05	20.0	18	41	4.1	0.91
2	0.45	0.05	20.0	25	43	4.3	2.3
3	0.40	0.05	20.0	29	62	11.6	2.4
4	0.45	0.05	20.0	20	38	5.0	1.3
5	0.45	0.05	20.0	25	89	4.8	3.0
6	0.60	0.05	20.0	23	96	4.1	2.5
7	0.43	0.05	20.0	24	51	4.9	2.4

$U_{\infty m}$ is the measured maximum fluid velocity above rippled bed.
Γ_{max} is the measured maximum value of vortex circulation.
C_m is the measured concentration of cloud.
A is the cross-sectional area of clouds when the concentration is measured.

The constants C_1 and γ_0 in Equations (9) and (10) can be fixed from the experiments. The constants are determined so that the measured and calculated situation of vortex center coincide when the flow direction is changed, i.e., main flow velocity is zero. Based on Equations (4), (5), (7), (9) and (10) with the estimated constants k_1, k_2, k_3, C_1 and γ_0, the

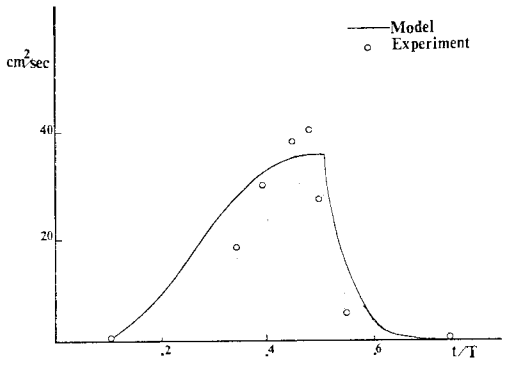

Fig. 4 Circulation of vortex (Case 1).

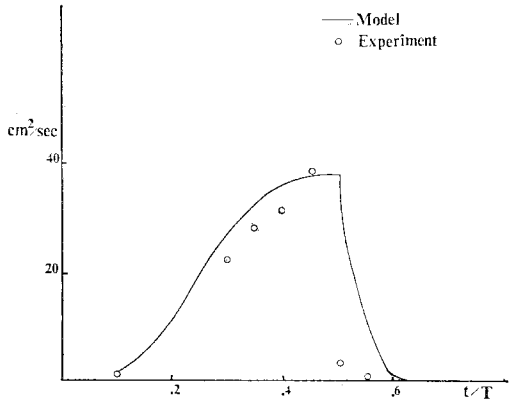

Fig. 5 Circulation of vortex (Case 4).

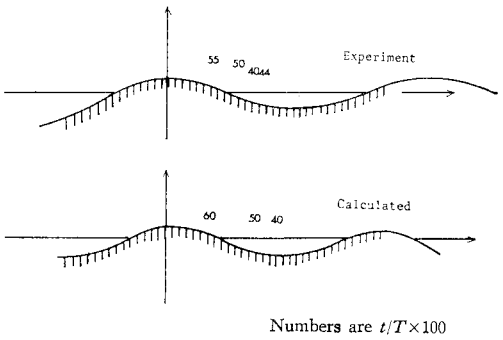

Fig. 6 Comparison between modeled and measured vortex center movement (Case 1).

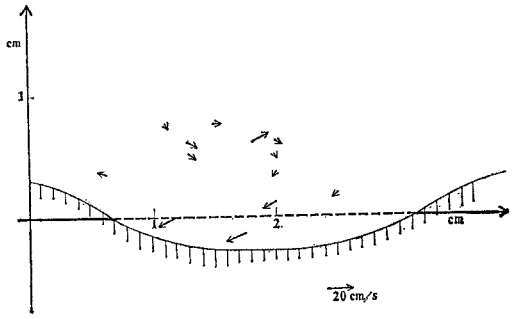

Fig. 7 (a) Calculated velocity field at the moment when the flow direction is changed (Case 4).

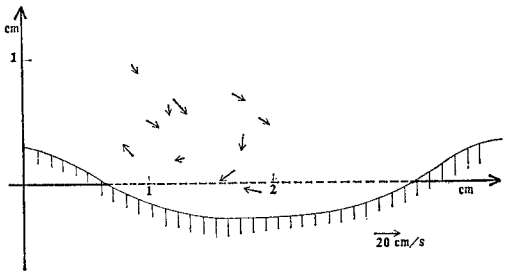

Fig. 7 (b) Measured velocity field at the moment when the flow direction is changed (Case 4).

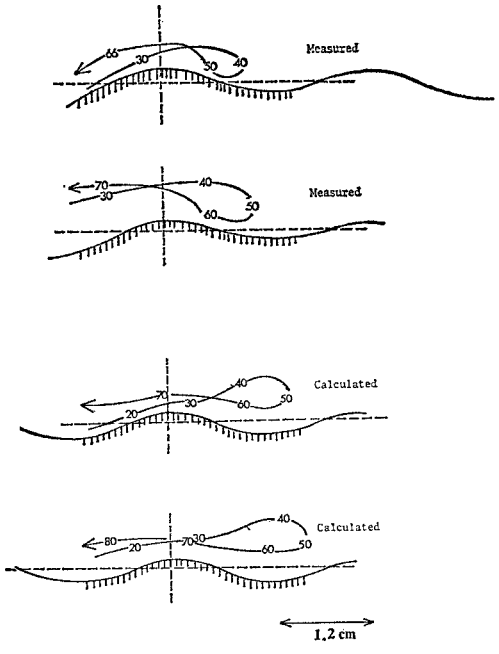

Numbers are $t/T \times 100$

Fig. 8 Comparison between calculated and measured water particle movement (Case 1).

velocity field over the flat boundary can be calculated. The quantities for the plane with a flat boundary are then transformed into those for a wavy

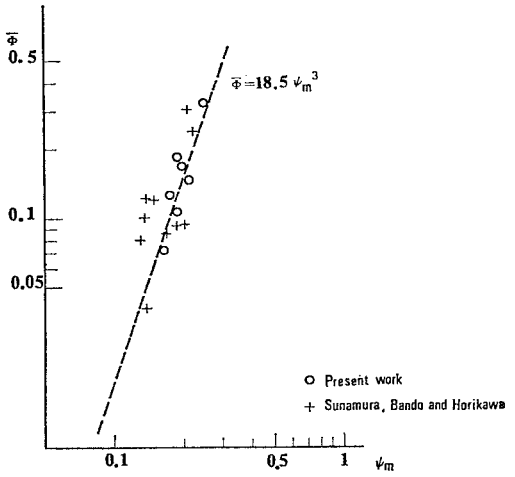

Fig. 9 Empirical relationship for rate of sand suspension due to waves.

boundary. Comparisons between the modeled and measured values of vortex center movement and velocity field over a rippled surface are shown in **Figs. 6** and **7** respectively.

The time integration of the velocity field at the plane with a flat boundary, after transforming into the wavy boundary, gives the pathlines of water particles over a rippled bed. The comparisons between measured and calculated pathlines are shown in **Fig. 8**, and good agreement is seen. This implies that the present model is applicable for predicting sand particle movement over a rippled bed when wave profile is reasonably approximated by a sinusoidal wave. When the effect of wave asymmetry is marked, the model should be modified by adopting non-linear wave theory.

The time average rate of sand suspension is calculated from the amount of suspended sand and wave period. The results for the time average rate of sand suspension are shown in **Fig. 9** together with the laboratory data of Sunamura, Bando and Horikawa[13]. The agreement between the proposed formula and the laboratory data is considered sufficiently good to justify the use of the present model.

3. NET RATE OF SEDIMENT TRANSPORT AND RESULTANT BEACH PROFILE CHANGE

(1) Model of net sediment transport

The transport types presented by Horikawa, Sunamura and Shibayama[4] are classified in terms of two parameters, ψ_m and u_b/w, where the quantity u_b/w is the ratio of maximum fluid velocity to sand particle fall velocity. Experimental results show that sand particles move at almost the same speed as water particles. The parameter u_b/w indicates

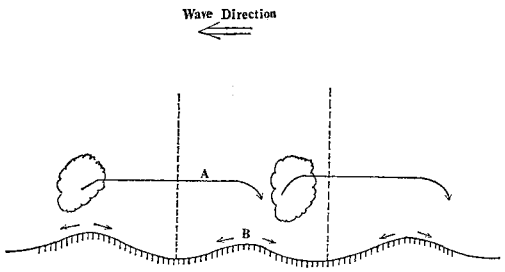

A : Suspended sand cloud movement results in a net sediment transport.
B : Rates of backward movement and forward movement are almost the same.

Fig. 10 A model of net sediment transport (Type 3).

how far a sand particle travels when suspended.

A suspended sand transport model is proposed for Type 3 and Type 4 transport under the following two assumptions based on laboratory observations;

1. The ripple length and the maximum excursion amplitude of water particle movement are of almost the same order, which means suspended sand clouds are transported over the distance of approximately one ripple length.
2. Ripple movement is very slow and its contribution to the net rate of sediment transport is negligible.

The present model is shown in **Fig. 10**. Back and forth movement is accomplished by wave action. Suspended sand clouds are transported for the distance of one ripple length in one wave period resulting in net sediment transport.

The amount of suspended sand is estimated by using Equation (23). The estimated net suspended sediment transport rate for unit time $\bar{\phi}_{sus}$ in the offshore direction is

$$\bar{\phi}_{\mathrm{sus}}=\bar{\phi}_{\mathrm{on}}\times\frac{T_{\mathrm{on}}}{T} \quad \cdots\cdots(24)$$

for Type 3 and

$$\bar{\phi}_{\mathrm{sus}}=\bar{\phi}_{\mathrm{on}}\times\frac{T_{\mathrm{on}}}{T}-\bar{\phi}_{\mathrm{off}}\times\frac{T_{\mathrm{off}}}{T} \quad \cdots\cdots(25)$$

for Type 4, where $\bar{\phi}_{\mathrm{off}}$ and $\bar{\phi}_{\mathrm{on}}$ indicate nondimensional sediment transport rates which are respectively given by Equation (23) during the offshore direction period T_{off} and the onshore direction period T_{on} respectively.

The bed load transport formula of Madsen and Grant[8] is adopted for Type 1 taking the bottom slope into consideration. Gravity acts in the down slope direction. The instantaneous value of the Shields parameter $\psi_b(t)$ including the influence of bottom slope may be expressed as the ratio of the entraining force to stabilizing force as

$$\psi_b(t)=\left[\frac{\left\{\frac{1}{2}f_w\rho u_b^2\sin^2\sigma t\frac{\pi}{4}d^2\right\}}{\left\{-\rho g(s-1)\frac{4}{3}\pi\left(\frac{d}{2}\right)^3\sin\beta\right\}}\right]\times\frac{2}{3}$$

$$=\psi_m\sin^2\sigma t-0.67\sin\beta \quad 0\leqq t/T\leqq\frac{1}{2} \quad \cdots\cdots(26)$$

$$\psi_b(t)=-\psi_m\sin^2\sigma t-0.67\sin\beta \quad \frac{1}{2}\leqq t/T\leqq 1 \quad \cdots\cdots(27)$$

in which

β=bottom slope angle

Hence

$$\bar{\phi}_{\mathrm{off}}=\int_0^{T/2}40\{\psi_b(t)\}^3dt$$

$$=12.5\,\psi_m{}^3-40.0\sin\beta\psi_m{}^2+54.4\sin^2\beta\psi_m-12.0\sin^3\beta \quad \cdots\cdots(28)$$

$$\bar{\phi}_{\mathrm{on}}=-12.5\,\psi_m{}^3-40.0\sin\beta\psi_m{}^2-54.4\sin^2\beta\psi_m-12.0\sin^3\beta \quad \cdots\cdots(29)$$

The net rate is given by

$$\bar{\phi}_{\mathrm{bed}}=\bar{\phi}_{\mathrm{off}}+\bar{\phi}_{\mathrm{on}} \quad \cdots\cdots(30)$$

Nonlinear wave theory is adopted to calculate the maximum and minimum fluid velocity. According to Madsen[7], when the Ursell parameter U_r given by,

$$U_r=\frac{HL^2}{h^3}$$

in which

H=wave height;

L=wave length;

h=water depth;

is greater than 26, cnoidal wave theory should be used. When the Ursell parameter is equal to or smaller than 26, Stokes second order theory is used.

For Type 2, the net transport rate is estimated as the weighted sum of the bed load formula and the suspended load formula.

$$\bar{\phi}_{\mathrm{net}}=2m\bar{\phi}_{\mathrm{sus}}+n\bar{\phi}_{\mathrm{bed}} \quad \cdots\cdots(31)$$

The coefficients m and n can be determined by the two parameters ψ_m and u_b/w from the laboratory experiments as will be discussed in the next section.

The estimated value of the net sediment transport rate and resultant beach profile change are compared with the laboratory data of Horikawa, Sunamura and Shibayama[4] and Horikawa, Sunamura and Kondo[3].

(2) Analysis of laboratory data

The experiments were performed by Horikawa, Sunamura and Shibayama[4] in a wave flume which is 25 m long, 0.8 m wide and 1.5 m deep. Similar experiments were performed by Horikawa, Sunamura and Kondo[3] in the same flume. Sand was positioned at an initial slope in the flume. Waves were generated at one end of the flume and the beach profile

change was recorded at regular time intervals. The various experimental conditions are shown in **Table 3**.

The models presented here are adopted to the offshore region for each case. The beach profile change is calculated from the dimensionless sediment transport rate as the change of mean sand level.

Two inspection sections are selected in offshore region whose locations are shown in **Figs. 12~14**. Then sediment transport formulae are adopted to the sections and the accretion or erosion rate is calculated from the differences between values of net sediment transport rate in two sections. During the experiment, breaking points move as beach profile changes as shown in **Figs. 12~14**.

Table 3 Experimental conditions for beach profile change.

Case Number	Deep Water Wave Height (cm)	Wave Period (s)	Initial Slope	Run Time (hr)	Sediment Diameter (cm)	Transport Type	Experiment
I	10.0	1.5	0.1	20	0.02	2, 3, 4	H-S-S
II	7.6	1.5	0.1	20	0.02	2, 3	H-S-S
III	7.6	1.0	0.1	160	0.02	[2, 3]	H-S-K
IV	7.6	1.0	0.05	160	0.02	[2, 3]	H-S-K
V	7.6	1.0	0.033	160	0.02	[2, 3]	H-S-K
VI	9.3	1.5	0.1	2	0.07	1	H-S-S
VII	7.5	2.0	0.1	2	0.07	1, 2	H-S-S

Sediment Specific Gravity=2.65
H-S-S=Horikawa, Sunamura and Shibayama[4]
H-S-K=Horikawa, Sunamura and Kondo[3]
[ ] means estimated value

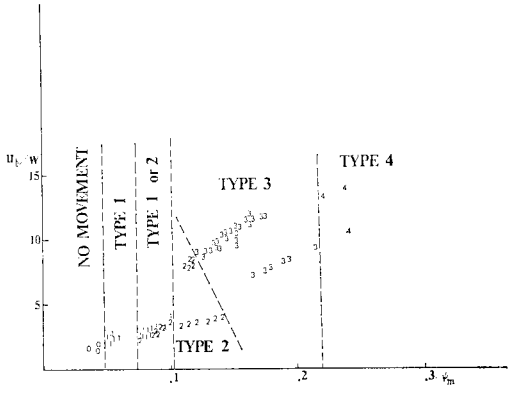

Fig. 11 Limits for each transport type.

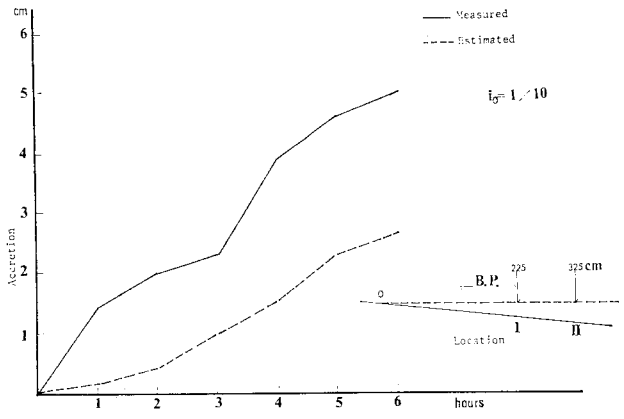

Fig. 12 Comparison between estimated and measured beach profile change (Case I).

(3) Results and discussion

Results indicate that the limits for each transport type are well described by the two parameters ψ_m and u_b/w as shown in **Fig. 11**.

Comparisons between the estimated and measured beach profile change are shown in **Figs. 12** through **14**. In spite of the restrictions due to the assumptions, for example slope effect is not considered in Types 2,3 and 4, the agreement between the proposed model and the laboratory data is considered enough to justify the validity of the present model as the first trial.

The coefficients m and n for Type 2 transport are decided by the ratio u_b/w. When u_b/w is greater than 7, $m=0.5$ and $n=0$ are adopted, which means suspended sand transport is dominant. When u_b/w is smaller than 4, $m=0$ and $n=1$ are taken, which means bed load transport is dominant. When u_b/w is between 4 and 7, $m=0.5$ and $n=1$ are proposed, which means onshore direction transport and offshore direction transport are almost equal and no net transport results.

The effect of bed slope on model for Types 3 and 4 transport has not been considered but is important. **Fig. 15** shows the effect of slope on the Type 3 model. The quantity $\bar{\phi}_m/\bar{\phi}_e$ is the ratio of measured net sediment transport rate to calculated one, where measured one is determined from the beach profile change.

When the slope is zero, which means the bed is not inclined, the, Type 3 model gives somewhat overestimated values due to two main reasons. First, Equation (23) is used to estimate the amount of suspended sand and it sometimes gives overestimation or underestimation of the amount of suspended sand. Second, we assumed that the suspended sand clouds are transported only in the offshore direction as discussed in Section 3-(1). But in the experimental phenomena, some part of the suspended sand does not fall to the bed, and is transported in the onshore direction. When the slope is gentle, that is bottom slope is 0.02~0.05, this model gives a good approximation. When the slope is steep, that is bottom slope is greater than 0.05, the effect of slope

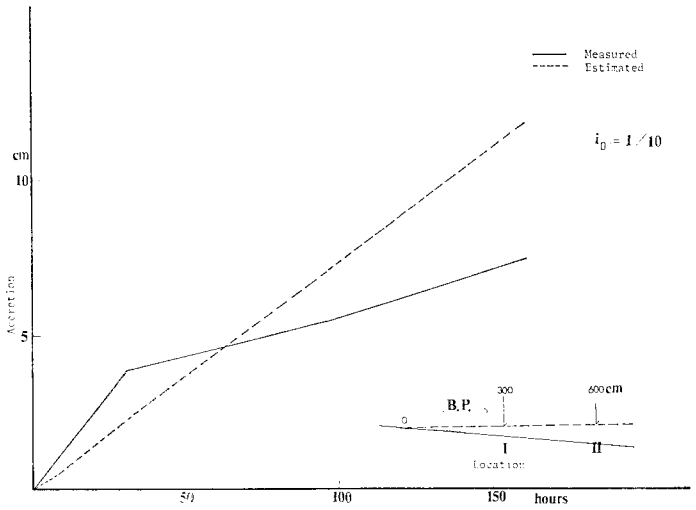

Fig. 13 Comparison between estimated and measured beach profile change (Case III).

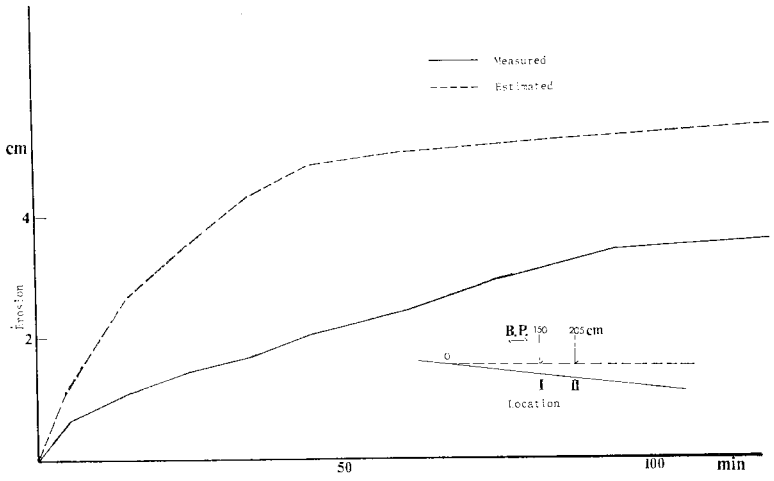

Fig. 14 Comparison between estimated and measured beach profile change (Case VI, Type 1).

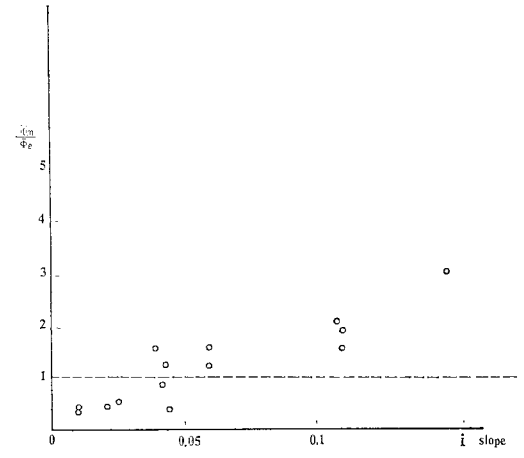

Fig. 15 Effect of slope on net sediment transport rate.

is significant and the model gives an underestimation. Gravity acts in the down slope direction and results net sediment transport in a down slope direction.

As a next stage, the effect of bottom slope should be quantitatively consiedred in the mo delsfor Typs 3 and 4 transport.

4. SUMMARY AND CONCLUSIONS

The present state of the art of predicting suspended sand movement due to wave action is far from satisfactory. Some experimental and model investigations were done in this study.

The present study reaches the following conclusions.

1) The movement of suspended sand is similar to that of a water particle and is well described by potential flow theory with the value of vortex circulation given from the present model.

2) The amount of suspended sand can be estimated with the application of a unidirectional flow bed load transported formula.

3) The types of sediment transport mechanisms can be classified with two parameters, the Shields parameter and the ratio of maximum fluid velocity to sediment particle fall velocity.

4) Different net sediment transport formulae are applied to each type of transport.

ACKNOWLEDGMENTS

The authors express their appreciation to Dr. A. Watanabe, Associate Professor, and Mr. M. Isobe, Research Associate, of the University of Tokyo for their fruitful discussions or suggestions. They are also grateful to Dr. N.C. Kraus of the Nearshore Environment Research Center for his assistance in the correction of the phraseology in the manuscript.

NOTATION

A_s : amount of moving sand as bed load transport

A_{sm} : maximum amount of moving sand as bed load transport
C_1 : constant indicating situation where flow separation occurs
d : sediment diameter
f : function expressing conformal transform
f_w : Jonsson's wave friction factor
g : gravity acceleration
g_1 : function expressing the relationship between Shields parameter and sediment transport rate
H : wave height
h : water depth
i_0 : initial bottom slope
K', K'', K''' : coefficients for model of circulation
k_1 : coefficient in integration of vorticity flux
k_2 : coefficient in decrease of circulation in positive flow direction
k_3 : coefficient in decrease of circulation in negative flow direction
k_T : ripple wave number
L : wave length
q_s : instantaneous volumetric rate of sediment transport
T : wave period or period of oscillation
T_{on} : period corresponding to onshore flow direction
T_{off} : period corresponding to offshore flow direction
t_i : time at which amount of sand in suspended sand cloud starts to increase
t_e : time at which amount of sand in suspended sand cloud attains maximum
U_∞ : oscillatory flow or wave motion free stream velocity
$U_{\infty m}$: maximum value of oscillatory flow or wave motion free stream velocity
u : x-component of fluid velocity
u' : ξ-component of fluid velocity
u_s : velocity of sand moving as bed load transport
u_{sm} : maximum velocity of sand moving as bed load transport
$\tilde{u}_0'$: ξ-component of velocity of vortex center movement
u_b : maximum fluid velocity relative to the bed
U_1 : Ursell parameter
v : y-component of fluid velocity
v' : γ-component of fluid velocity
$\tilde{v}_0'$: γ-component of velocity of vortex center movement
W_0 : complex number indicating the location of real vortex in the plane with flat boundary
$\overline{W}_0$: complex number indicating the location of image vortex in the plane with flat boundary
w : fall velocity for a sediment particle
x, y : coordinates in the plane with wavy boundary
α : ripple amplitude
α_1 : coefficient in time at which suspended sand cloud starts to increase
β_1 : coefficient in time at which suspended sand cloud stops to increase
β : bottom slope angle
γ_0 : γ-component of vortex center
ξ, γ : coordinates for the plane with flat boundary
ξ_0 : ξ-component of vortex center
Ω : complex potential for the plane with flat boundary
$\tilde{\Omega}$: complex potential for the plane with flat boundary when real vortex is eliminated
ρ : density of fluid
σ : radian wave frequency
ϕ : non-dimensional sediment transport rate
$\bar{\phi}$: time averaged dimensionless sediment transport
$\bar{\phi}_{net}$: time averaged dimensionless net sediment transport
$\bar{\phi}_{off}$: time averaged dimensionless offshore direction sediment transport
$\bar{\phi}_{on}$: time averaged dimensionless onshore direction sediment transport
$\bar{\phi}_e$: estimated time averaged dimensionless net sediment transport rate
$\bar{\phi}_m$: measured time averaged dimensionless net sediment transport rate
$\bar{\phi}_{sus}$: time averaged dimensionless suspended sediment transport rate
$\bar{\phi}_{bed}$: time averaged dimensionless bed load sediment transport
Γ : circulation of vortex
τ_{0m} : bottom shear stress based on the maximum near bottom fluid velocity
ψ : Shields parameter
ψ_m : Shields parameter based on the maximum value of the bottom shear stress
ψ_b : Shields parameter with influence of bottom slope

REFERENCES

1) Brown, C.B. : Sediment Transport, In : Rouse H.Ed., Engineering Hydraulics, John Wiley and Sons, Inc., N.Y., pp. 1039, 1950.
2) Einstein, H.A. : A Basic Description of Sediment Transport on Beaches, In : Waves on Beaches and Resulting Sediment Transport, Academic Press, New York, pp. 53~93, 1972.
3) Horikawa, K., T. Sunamura and Y. Kondo : Labora-

tory Study on Two Dimensional Beach Profile Change, Proc. 21st Conf. on Coastal Engineering in Japan, pp. 193～199, 1974 (in Japanese).

4) Horikawa, K., T. Sunamura and T. Shibayama : Experimental Study of Two-Dimensional Shore Transformation, Proc. 24th Conf. on Coastal Engineering in Japan, pp. 170～174, 1977 (in Japanese).

5) Inman, D.L. : Wave Generated Ripples in Nearshore Sands, Beach Erosion Board, Tech. Memo., No. 100, 1957.

6) Jonsson, I.G. : Wave Boundary Layers and Friction Factors, Proc. 10th Conf. on Coastal Engineering, ASCE, Vol. 1, pp. 127～148, 1966.

7) Madsen, O.S. : On the Generation of Long Waves, Journal of Geophysical Research, Vol. 76, No. 36, pp. 8672～8683, 1971.

8) Madsen, O.S. and W.D. Grant : Sediment Transport in the Coastal Environment, Report No. 209, Ralph M. Parsons Laboratory for Water Resources and Hydrodynamics, Dept. of Civil Engineering, MIT, 1976.

9) Nakato, T., F.A. Locher, J.R. Glover and J.F. Kennedy : Wave Entrainment of Sediment from Rippled Beds, Journal of the Waterways, Harbors, Coastal and Ocean Engineering Division, ASCE. Vol. 103, No. WW 1, pp. 83～99, 1977.

10) Ringleb, F.O. : Separation Control by Trapped Vortices, Boundary Layer and Flow Control, Pergamon, New York. Vol. 1, pp. 265～294, 1961.

11) Shibayama, T. : Laboratory Study on Sand Suspension over Ripples due to Wave Action, thesis presented to the University of Tokyo, in 1979, in partial fulfillment of the requirements for the Master of Engineering.

12) Sleath, J.F.A. : Measurements of Bed Load in Oscillatory Flow, Journal of the Waterways, Harbors, Coastal and Ocean Engineering Division, ASCE, Vol. 104, No. WW 4, pp. 291～307, August, 1978.

13) Sunamura, T., K. Bando and K. Horikawa : Experimental Study of Sand Movement and Transport over Asymmetrical Ripples, Proc. 25th Conf. on Coastal Engineering in Japan, pp. 250～254, 1978 (in Japanese).

14) Svendsen, Ib.A. : Cnoidal Waves over a Gently Sloping Bottom, Series Paper No. 6, Institute of Hydrodynamics and Hydraulic Engineering, Technical University of Denmark, 1974.

15) Tunstall, E.D. and D.L. Inman : Vortex Generation by Oscillatory Flow over Rippled Surfaces, Journal of Geophysical Research, Vol. 80, No. 24, pp. 3475～3484, 1975.

16) Yamaguchi, S. and M. Sawamoto: Estimation of Sand Concentration above Ripples due to Wave Action, Proc. 33rd Conf. of JSCE, Vol. 2, pp. 816～817, 1978 (in Japanese). also, Sawamoto, M. and Yamaguchi, S. : "Theoretical Modeling on Wave Entrainment of Sand Particles from Rippled Bed", Proc. of J.S.C.E., No. 288, pp. 107～113, Aug., 1979 (in Japanese).

17) Inman, D.L. and A.J. Bowen : Flume Experiments on Sand Transport by Waves and Currents, Proc. 8th Conf. on Coastal Engg., pp. 137～150, 1963.

(Received March 29, 1979)